Journal of Materials Science: Materials in Engineering

ORIGINAL PAPER

Open Access

Concentration modulated microstructure and rheological properties of nanofibrous hydrogels derived from decellularized human amniotic membrane for 3D cell culture

Golara Kafili[1], Elnaz Tamjid[2], Hassan Niknejad[3] and Abdolreza Simchi[1,4,5*]

Abstract

Decellularized amnion (dAM)-derived hydrogels have been extensively exploited for versatile medical and therapeutical applications, particularly for soft tissue engineering of skin, vascular graft, and endometrium. In contrast to polyacrylamide-based hydrogels, which have been extensively employed as a 3D cell culture platform, the cell response of dAM hydrogel is yet to be understood. In this study, we have prepared hydrogels containing different concentrations of dAM and systematically investigated their microstructural features, gelation kinetics, and rheological properties. The results show that dAM hydrogels possess a network of fibers with an average diameter of 56 ± 5 nm at 1% dAM, which increases to 110 ± 14 nm at 3% dAM. The enhanced intermolecular crosslinking between the microfibrillar units increases the gelation rate in the growth phase of the self-assembly process. Moreover, increasing the concentration of dAM in the hydrogel formulation (from 1 to 3%w/v) enhances the dynamic mechanical moduli of the derived hydrogels by about two orders of magnitude (from 41.8 ± 2.5 to 896.2 ± 72.3 Pa). It is shown that the variation in the hydrogel stiffness significantly affects the morphology of dermal fibroblast cells cultured in the hydrogels. It is shown that the hydrogels containing up to 2%w/v dAM provide a suitable microenvironment for embedded fibroblast cells with spindle-like morphology. Nevertheless, at the higher concentration, an adverse effect on the proliferation and morphology of fibroblast cells is noticed due to stiffness-induced phenotype transformation of cells. Concentration-modulated properties of dAM hydrogels offer an in vitro platform to study cell-related responses, disease modeling, and drug studies.

Keywords Decellularized extracellular matrix, Nanofibrous polymeric network, Injectable hydrogel, Cell culture

*Correspondence:
Abdolreza Simchi
simchi@sharif.edu
Full list of author information is available at the end of the article

Springer Open

© The Author(s) 2024. **Open Access** This article is licensed under a Creative Commons Attribution 4.0 International License, which permits use, sharing, adaptation, distribution and reproduction in any medium or format, as long as you give appropriate credit to the original author(s) and the source, provide a link to the Creative Commons licence, and indicate if changes were made. The images or other third party material in this article are included in the article's Creative Commons licence, unless indicated otherwise in a credit line to the material. If material is not included in the article's Creative Commons licence and your intended use is not permitted by statutory regulation or exceeds the permitted use, you will need to obtain permission directly from the copyright holder. To view a copy of this licence, visit http://creativecommons.org/licenses/by/4.0/.

Graphical abstract

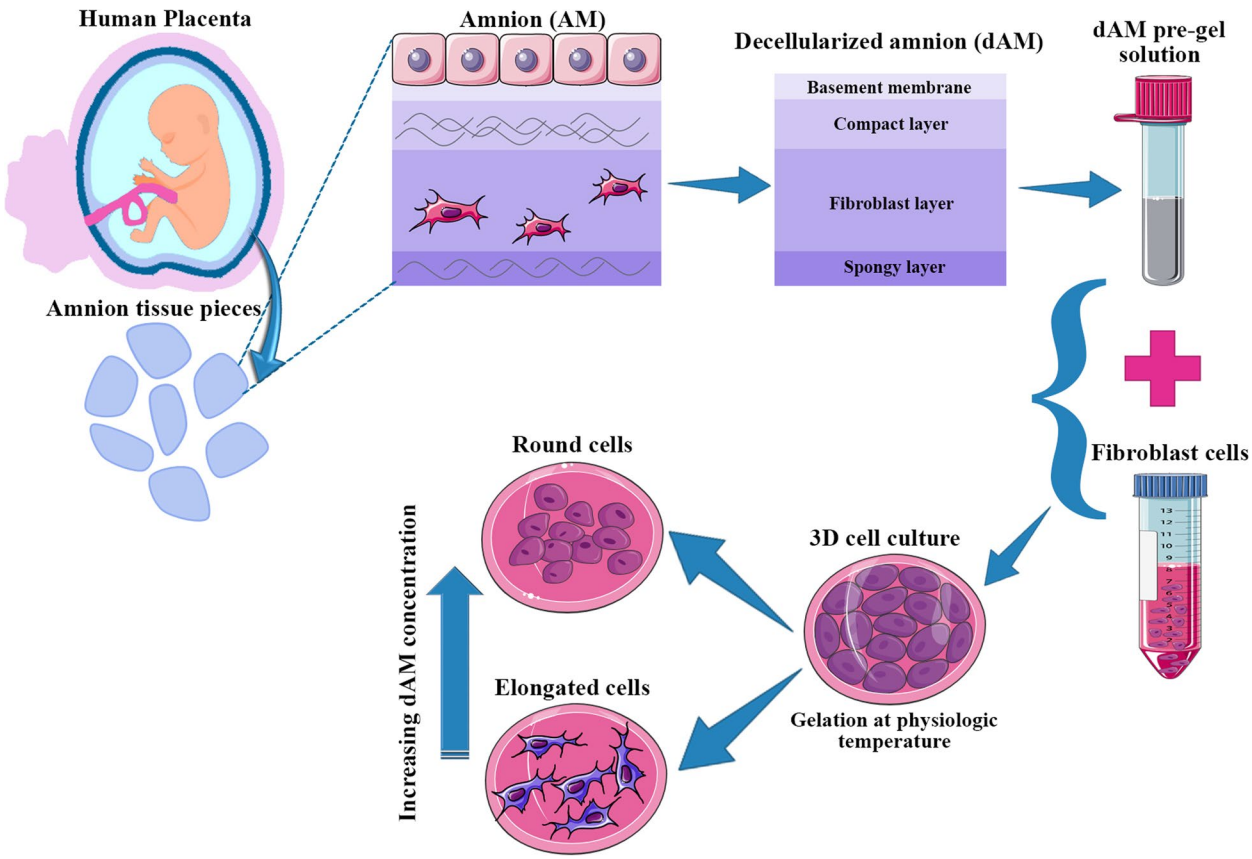

Introduction

The extracellular matrix (ECM) of tissues/organs comprises complex macromolecular substances secreted by various cell types in tissues and organs of the body that play a regulatory function in cellular behaviors, including cell growth, proliferation, differentiation, and migration (Zhang et al. 2021a). ECM is a tissue-specific microenvironment that consists of a very complex combination of different proteins, glycosaminoglycans, and growth factors (Saldin et al. 2017). Hence, the recapitulation of an exact ECM composition of the target tissue by combining various biopolymers and biomolecules is a challenging process (Sasikumar et al. 2019). As a result, processing decellularized extracellular matrix (dECM) by removing cellular components from tissues and organs has been considered an alternative method to provide a biomaterial resembling the natural niche of cells in a particular tissue (Jones et al. 2022).

Despite the bioactivity of decellularized tissues, the clinical applications of these biomaterials have faced serious limitations regarding matching geometrical and mechanical features (Zhang et al. 2021a). To overcome the limitations, recently temperature-sensitive dECM-derived hydrogels have been prepared by enzymatic digestion of dECM biomaterial in a mildly acidic solution followed by neutralization and incubation at physiological temperature (i.e., 37 °C) (Kafili et al. 2023a). Studies have shown that the injectability of dECM-derived pre-gel solution ensures its easy administration into the desired shaped defect site, while the temperature sensitivity of the hydrogel provides the required stability to remain immobile by gelation at the body temperature (Li et al. 2022). Nevertheless, there are still many synthesis parameters, including pH, ionic strength, concentration, and digestion time that have to be finely adjusted to prepare dECM-derived hydrogels with desirable properties (Saldin et al. 2017). Johnson and colleagues have shown that increasing the salt concentration from 0.5× to 1.5× PBS increases the gelation time of myocardial-derived hydrogels from 20 min to over 8 h (Johnson et al. 2011). It has also

been demonstrated that the majority of ECM components are solubilized after 24 h (Pouliot et al. 2020). Under this circumstance, the highest storage modulus is attained due to the branched and interconnected structure of the hydrogel. Further increasing the digestion time decreases the mechanical durability, demonstrating that the gelation process of dECM-derived hydrogels is more complex than the frequently used collagen hydrogels, most probably due to the active participation of other ECM components in the fibrillogenesis (Fernández-Pérez and Ahearne 2019). We have recently reported the effect of pepsin digestion time on the structural and rheological properties of decellularized amnion (dAM)-derived hydrogels (Kafili et al. 2023b).On the other hand, dECM-derived hydrogels have been considered an alternative and promising platform for 3D cell culture due to their cell-binding motifs and bioactive constituents (Ravichandran et al. 2021). However, despite their advantages over synthetic biomaterials, e.g., polyacrylamide-based hydrogels, concerning physiological relevance to cell behavior similar to in vivo conditions (Caliari and Burdick 2016; Chaudhuri 2017), the inferior mechanical properties of dECM-derived hydrogels limit their application as a 3D cell culture platform (Behan et al. 2022).

Human amnion (HAM) is an easy-to-access and low-cost tissue source with outstanding biological properties such as biocompatibility, low immunogenicity, anti-scarring, anti-inflammatory, and antibacterial effects that enable its clinical applications, especially for ocular regeneration and treatment of burn wounds (Doudi et al. 2022). In recent years, dAM-derived hydrogels have shown promising outputs for a broad range of biomedical applications such as skin repair (Zhang et al. 2021b; Kafili et al. 2024a). vascular grafts (Peng et al. 2020; Cheng et al. 2021), osteoarthritis treatment (Bhattacharjee et al. 2022, 2020), endometrium regeneration (Li et al. 2022), and heart tissue repair (Henry et al. 2020). To the best knowledge of the authors, a few research have been conducted so far on the application of dAM hydrogels for cell culture purposes. Ryzhuk et al. have shown that dAM hydrogels can be utilized as a cell carrier vehicle for stem cell therapy with characteristics compatible with other standard biomaterials, such as collagen and fibrin hydrogels (Ryzhuk et al. 2018). Deus et al. have prepared methacrylated dAM hydrogel (AdECMMA), as a versatile cell culture platform, by changing the methacrylation degree (Deus et al. 2022). The resulting photo-crosslinkable AdECMMA hydrogels are usable for 3D cell culture and regulating cell alignment by providing nano- or micro-topographical features. Nevertheless, UV light-induced cell death through DNA damage remains a great challenge for photocrosslinking hydrogel systems (Nieto et al. 2020). Moreover, the methacrylation process is prone to diminish the bioactivity of dECM hydrogels. Rottrauff et al. have compared the bio-functionality of thermally crosslinked decellularized cartilage-derived hydrogels (CdECM) with photocrosslinked methacrylated decellularized cartilage-derived hydrogels (CdECMMA) (Rothrauff et al. 2018). Their results suggest that CdECMMA hydrogels compromise the chondrogenic differentiation of seeded mesenchymal stem cells (MSCs) assessed by gene expression, matrix synthesis, and histological observations. Therefore, the thermally crosslinked dECM hydrogels are a better alternative for methacrylated counterparts in terms of preservation of bioactive components and providing a tissue-specific microenvironment.

The dECM hydrogels are also a valuable biomimetic platform for in vitro studies to resemble pathological conditions and to investigate cell-related responses (Kafili et al 2024b). Tunable and controllable in vitro platforms are indeed useful tools and microenvironments for exploring phenomena related to tissue regeneration and underlying disease mechanisms (Chan and Mooney 2008). Most of the tissues obtained from animal sources may not replicate human-specific microenvironments to predict human cell responses precisely. In this scenario, HAM is a rare human tissue that is available and does not face intense regularities for its clinical applications, owing to its inherent low immunogenicity that prevents the risk of transplant rejection (Niknejad et al. 2008). Therefore, the dAM hydrogels derived from human sources offer a great opportunity for studying human diseases, such as cancer progression and drug responses. The elaboration of such an in vitro model with the capability of mimicking different ranges of mechanical stiffness is highly useful and essential. To the best of our knowledge, the development of thermally crosslinked dAM hydrogels with tunable properties for 3D culture to investigate phenotypic and morphological changes of cells in response to matrix stiffness remains unexplored and warrants further investigation.

This study aims to prepare injectable hydrogels based on decellularized HAM through the self-assembly of collagen fibers within dECM. The different steps of the developed procedure to prepare the injectable hydrogel, evaluate the physicomechanical properties, explore biocompatibility, 3D cell culturing potential, and widen tissue engineering applications are shown in Fig. 1. The novelty of the work relates to the dAM concentration-modulated procedure that finely tunes the properties of the hydrogel, making it suitable for biomedical applications. We have systematically investigated the effects of dAM concentration on the structure, gelation kinetics, rheological properties, and cell

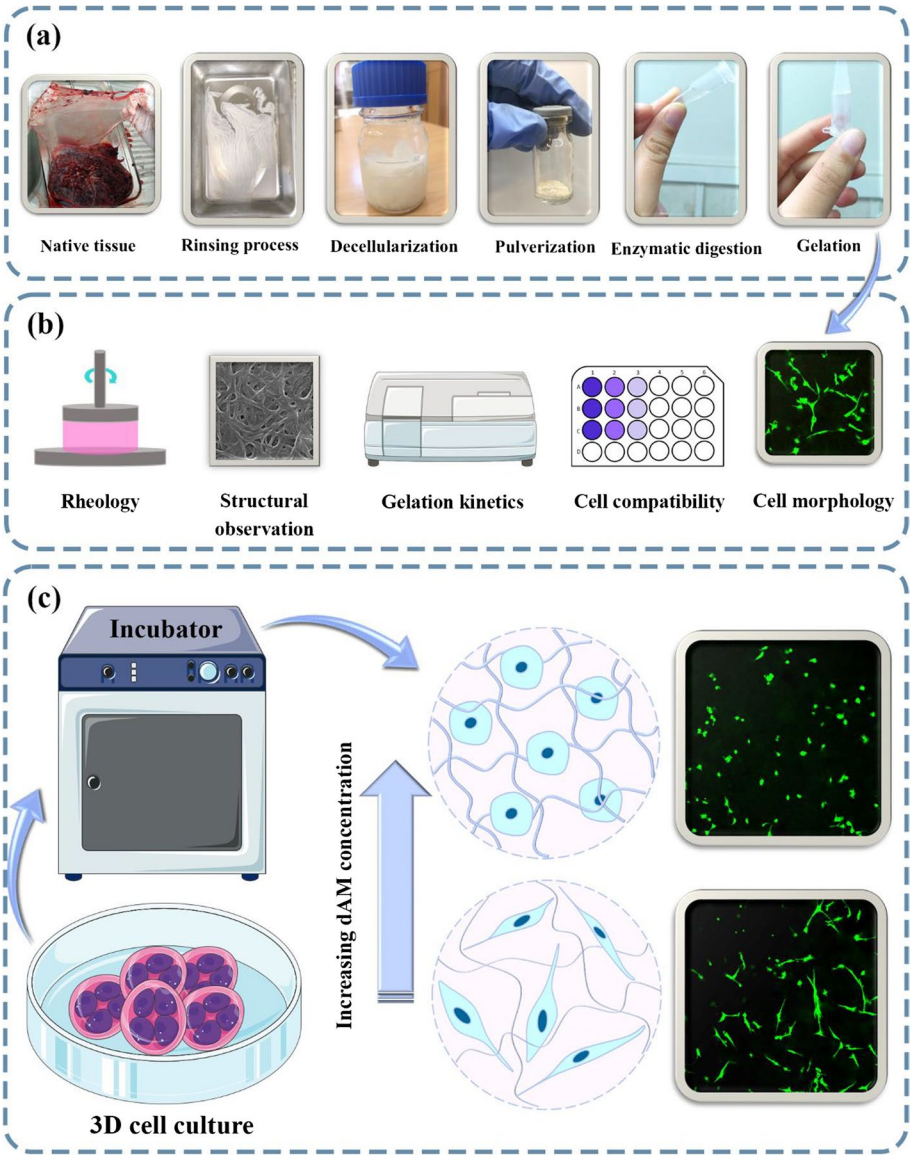

Fig. 1 Preparation of injectable hydrogel derived from dAM tissue. **a** The preparation steps include manual separation of AM from chorion, rinsing blood clots, decellularization, lyophilization and grinding, enzymatic digestion, and temperature-sensitive gelation of neutralized pre-gel solution at 37 °C. **b** Evaluated properties of dAM hydrogels for 3D cell culture. **c** The developed dAM hydrogel with tunned composition supports the 3D culture of cells and is useful for the mechanistic study of cells and tissue engineering applications

response of prepared hydrogels. It is shown that the mechanical properties of dAM hydrogel can be tuned by the concentration of dAM, which ultimately affects the fibroblast cell response, including viability, proliferation, and morphology. The results have important implications for the potential of dAM hydrogels as a platform for studying cellular behaviors in response to environmental factors, such as matrix mechanics.

Materials and methods

Materials

Pepsin enzyme, MTT assay kit, Ethylenediaminetetraacetic acid (EDTA), Triton X-100, NaOH, and glutaraldehyde were obtained from Sigma–Aldrich (USA). Penicillin/streptomycin antibiotic, trypsin/EDTA, fetal bovine serum (FBS), and dimethyl sulfoxide (DMSO) were purchased from Bioidea company (Iran). Dulbecco's

Modified Eagle's medium (DMEM) was acquired from Gibco (USA).

Preparation of dAM-derived hydrogels

A schematic representation of dAM processing to fabricate injectable temperature-sensitive hydrogels is shown in Fig. 1a. The details of processing and characterization methods are explained below.

Decellularization of AM tissue

This study was conducted based on the ethical code of IR.SBMU.AEC.1402.024 approved by the ethics committee of Shahid Beheshti University of Medical Sciences (Tehran, Iran). The human placentas were collected from consent parents undergoing elective Cesarean delivery at Babak Hospital (Tehran, Iran). All healthy mothers were screened for negative results of infectious diseases, including human immunodeficiency virus, hepatitis virus type B and type C, and syphilis. Immediately after birth, the placentas were collected and transported to the laboratory in an ice package. The decellularization process was carried out according to our recently published protocol (Kafili et al. 2023c). Briefly, AM was separated from the chorion membrane and rinsed in PBS to remove blood clots. The tissue was cut into approximately 4 cm^2 pieces and treated with 0.2%w/v EDTA solution for 2 h at 37 °C. After washing with PBS to remove cell fragments, the tissue pieces were incubated in 1%v/v Triton X-100 for 30 min at room temperature (RT). The decellularized tissues were washed with PBS three times. Lyophilization was carried out by an Alpha 2,4 Martine Christ freeze drier (Germany) at − 50 °C for 48 h. The obtained tissues were then grounded using a cryomilling device (Asia Fanavar Pars, Iran) for 10 min.

Digestion and gelation

For the preparation of a pre-gel solution, the dAM powder was digested in 0.01 M HCl supplemented with 10%w/w pepsin for 72 h. The solution was then neutralized by using a NaOH solution (10 N). The concentration of dAM in the hydrogel formulation was adjusted to 1, 2, and 3%w/v (denoted as AM1, AM2, and AM3, respectively), and gelation was carried out by incubating neutralized dAM pre-gel solutions at 37 °C for 60 min to let the thermal crosslinking take place.

Histological examination of dAM tissue

To check the quality of the decellularization process, the content of DNA, collagen, and GAG was qualitatively compared to the native AM tissue. The samples were histologically stained with hematoxylin and eosin (H&E), Masson's trichrome (MT), and alcian blue (AB) to reveal the remnant cell components, collagen, and GAGs, respectively.

Materials characterizations

Rheological studies

Rheological properties of hydrogels were measured using an Anton Paar rheometer (MCR300 model, Austria) equipped with a 25 mm parallel plate geometry. To check the gelation kinetics, time sweep measurements at a strain of 1% and a frequency of 1 Hz were conducted. The temperature was swept from 4 to 37 °C with a rate of 5 °C/min and finally incubated at 37 °C for 60 min. The moduli were determined from the dynamic frequency sweep test in the range of 10^{-2}–10^{2} Hz at a constant strain of 1%. A steady shear sweep analysis in the range of 10^{-2}–10^{3} s^{-1} was conducted to evaluate the flow behavior. The obtained viscosity (η)-shear rate (γ) curves were fitted with the well-known power law rheological model (Eq. 1) to determine the flow consistency index (k) and shear thinning index (n) (Peak et al. 2018).

$$\eta = k\gamma^{n-1} \tag{1}$$

Gelation kinetics

The turbidimetric assay was applied for the investigation of gelation kinetics. One hundred microliter/well of each neutralized pre-gel solution was added into a 96-well plate and incubated at 37 °C using a BioTek microplate reader (PowerWave XS model, USA). The optical density of samples was recorded at 405 nm every 2 min for an overall 40 min, and the normalized absorbance (NA) was determined by:

$$NA = \frac{A - A_0}{A_{max} - A_0} \tag{2}$$

where A_0, A, and A_{max} are the initial absorbance, the absorbance at a given time, and the maximum absorbance, respectively. The kinetic parameters of half-time of gelation ($t_{1/2}$), lag time (t_{lag}), and gelation rate were extracted from gelation curves, as described in the literature (Fernández-Pérez and Ahearne 2019).

Microscopy

The tissue pieces and crosslinked hydrogels were fixed using a 2.5%v/v glutaraldehyde solution, washed with PBS, and dehydrated using a rising series of ethanol solutions (30 to 100%). After gold sputtering, the ultrastructure of samples was observed by scanning electron microscopy (VEGA, TESCAN, Czech Republic) at 15 kV.

Spectroscopy

Fourier transform infrared (FTIR) spectroscopy was conducted in the wavenumber range of 400 to 4000 cm^{-1} using a Tensor 27 spectrophotometer (Bruker, Germany).

In vitro biological assays

Cell culture

Human dermal fibroblast cells (HDFs) were purchased from the Pasteur Institute (Tehran, Iran). HDFs were cultured in DMEM supplemented with 10% FBS and 1% antibiotic. After reaching ~ 80% confluency, the cells were detached after incubation with 0.25% trypsin/EDTA for 3 min and collected by centrifugation at 1500 rpm for 5 min. Finally, the cells were counted and resuspended to obtain the desired cell density.

Cytocompatibility

The in vitro biocompatibility of the hydrogels was assessed using an indirect MTT assay according to the ISO10993-5 standard. The pre-gel solutions were placed into 24-well plates and incubated for 60 min at 37 °C. Sterilization was done by soaking in 70% ethanol solution overnight, and washing with sterile deionized (DI) water, followed by UV exposure for 30 min. A complete cell culture medium was then added to each well and incubated for 1, 4, and 7 days at 37 °C. At each time interval, the medium was removed and used as the extraction. Cells with a density of 10^4 cells/well were seeded in 96-well plates and incubated for 24 h. Then, the medium was replaced by the extraction medium (100 µl) and incubated for 24 h. Cells treated with a complete DMEM medium were considered the control group. Next, the extracts were removed, and 100 µl of 0.5 mg/ml MTT solution was added to each well and incubated for 4 h. To dissolve formazan crystals, the MTT solution was aspirated and the samples were incubated with 100 µl DMSO for 30 min. The absorption of the solutions at 570 nm was measured using the LEDETECT 96 microplate reader. The cell viability was calculated using the following equation:

$$Viability(\%) = \frac{A_s - A_b}{A_c - A_b} \times 100 \quad (3)$$

where A_s, A_c, and A_b are the absorbance values of experimental samples, control, and blank groups, respectively.

Live/dead assay

To directly assess the effect of dAM content on cell viability, HDFs with a density of 1×10^6 cells/ml were encapsulated in the hydrogels with the final concentrations of 1, 2, and 3%w/v. Gelation of the cell-encapsulated hydrogels (100 µl/well) was carried out in a 24-well plate through 60 min incubation at 37 °C. Then, the complete fresh medium was added to wells, and the samples were cultured for up to 7 days. The culture medium was changed three times a week. The viability of encapsulated cells after day 1 and day 7 was checked using a live/dead assay kit (ThermoFisher Scientific, USA). At the pre-defined time points, the hydrogels were incubated in 4 mM Calcein-AM and 2 mM ethidium homodimer for 30 min followed by several washing steps with PBS. The images of live cells (green color) and dead cells (red color) were captured by a confocal microscope (Nikon Instruments, C2 model, Japan). The cell spreading area and cell circularity factor were calculated using the Digimizer image analyzer software (version 5.4.9).

Statistics

Three replicates were considered for each experiment, and the results were reported as mean ± standard deviation (SD). The one-way analysis of variance (ANOVA) followed by Tukey's multiple comparison tests was carried out by employing Graphpad Prism software (Version 9.2.0 (332)). A p-value < 0.05 marked with (*) was considered significantly different.

Results

Evaluation of decellularized tissue

SEM studies have indicated that the native AM tissue represents a plumpy and cobblestoned morphology of epithelial cells (Fig. 2a). After decellularization, the tissue exhibits a nanofibrous network structure with an average fiber diameter of 72.0 ± 3.0 nm (Fig. 2a). No sign of residual cells on the tissue is noticed. Histological studies (H&E staining) also affirm the successful removal of cells (Fig. 2b). In addition, the MT and AB staining determines collagen (Fig. 2c) and GAG (Fig. 2d) within the dAM matrix. Preservation of these biomolecules is a critical element for the bio-functionality of the processed tissue, including cell signaling for cellular activities such as cell adhesion and proliferation (Zhang et al. 2016).

Microstructure and chemical composition of dAM hydrogels

FTIR spectra of AM and dAM tissues as well as dAM hydrogel composition are shown in Fig. 3a. The main peaks in the AM tissue include the stretching vibration of O–H and N–H bonds (amide A) at 3342 cm^{-1}, N–H bending vibration (amide B) at 3068 cm^{-1}, C=O stretching mode (amide I) at 1645 cm^{-1}, bending of N–H groups (amide II) at 1534 cm^{-1}, pyrrolidine rings of amino residues of proline and hydroxyproline at 1454 cm^{-1}, and C–N stretching and N–H bending (amide III) at 1320 cm^{-1} (Sripriya and Kumar 2016). These characteristic peaks as collagen fingerprints affirm the presence of collagen as the main component of AM

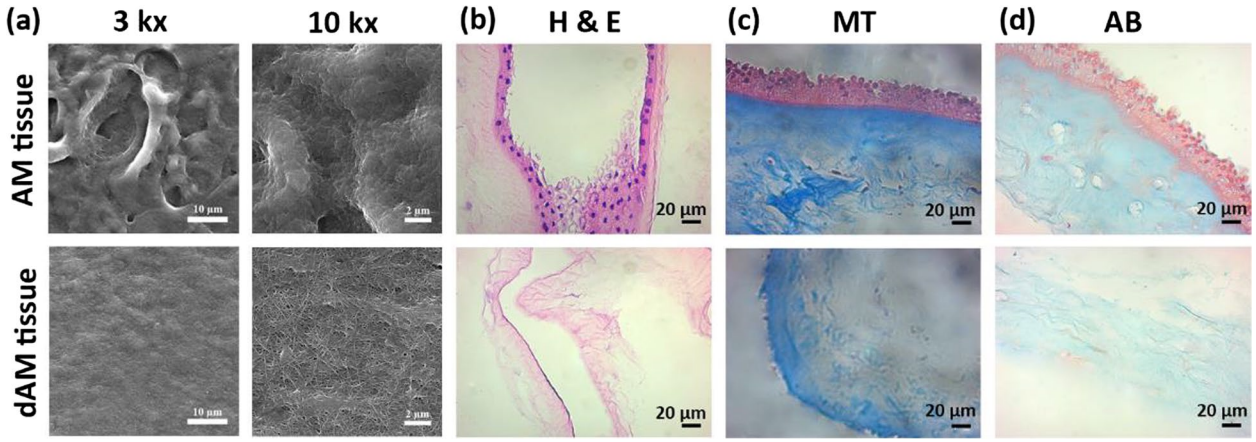

Fig. 2 Evaluation of the decellularization process. **a** Representative SEM images of AM tissues before and after decellularization at two different magnifications (scale bars are 10 µm and 2 µm, respectively). Histological examination of AM and dAM tissues for qualification of **b** cells removal by hematoxylin and eosin (H&E) staining, **c** collagen presence by Masson's trichrome (MT) staining **c**, and **d** remaining GAG by alcian blue (AB) staining

tissue. Two bands at 2931 and 2860 cm^{-1} correspond to the asymmetric and symmetric stretching vibration of C–H bonds. The peaks located at 1399 and 630 cm^{-1} are ascribed to the carboxylate and C=O planar deformation of amide IV, respectively (Cavalu et al. 2021). The absorbance peaks at 682 cm^{-1} and 1150 cm^{-1} are attributed to the out-of-plane N–H wagging of the amide group and O–C bands, respectively (Villamil Ballesteros et al. 2020). The peak at 1062 cm^{-1} is assigned to the presence of glycosaminoglycans (GAGs) (Toniato et al. 2020), while that at 1237 cm^{-1} signifies the S=O stretching vibration of polysaccharides in the AM matrix (Bhattacharjee et al. 2020). The location of amide peaks in the FTIR spectrum of dAM tissue does not show a significant shift, implying the preservation of collagen after the decellularization process (Sripriya and Kumar 2016). Other studies on the extraction of collagen from different tissues (e.g., skin tissue) correlate the preservation of the peak at 1645 cm^{-1} to the integrity of the triple helix structure of collagen (Toniato et al. 2020). Hence, it can be deduced that the adopted decellularization method in this work does not harm the structural features of collagen content within the dAM matrix. Nevertheless, some of the ECM components are likely lost during the decellularization process, as evidenced by disappearing bands in the dAM spectrum, particularly within the lower range of wavenumbers. Although the FTIR spectrum of the dAM hydrogel exhibits the main absorbance peaks of collagenous components, their intensities are weaker as caused by the enzymatic digestion during the solubilization process.

By employing thermal crosslinking, hydrogels with different dAM concentrations (1, 2, and 3%w/v) were prepared. Representative SEM images showing their structure are presented in Fig. 3b. The AM1 and AM2 hydrogels exhibit a nano-fibrillar morphology with random orientations, which can be favorable for cell permeability (Chao et al. 2022). The AM3 hydrogel shows a thick fibrous structure with aggregated nodes. The formation of fiber bundles occurs through the aggregation of fibril filaments at high concentrations of dAM (Tian et al. 2021). The box plot of fiber size distribution is shown in Fig. 3c. The average fiber diameter for the AM1 hydrogel is 56.0 ± 5.0 nm which increases to 75 ± 5.0 nm and 110 ± 14 nm by increasing the dAM concentration to 2%w/v and 3%w/v, respectively. It is noteworthy that the AM1 hydrogel also possesses some tiny fibrils with a diameter of 20–40 nm, which is not observed in hydrogels with higher concentrations. Among the various examined dAM concentrations, the AM2 hydrogel demonstrates the most resemblance to the native decellularized AM tissue, as shown in Fig. 2a.

Viscoelastic behavior and rheological properties

To evaluate the temperature sensitivity of dAM hydrogels, a time sweep rheological analysis comprising a temperature ramping from 4 to 37 °C and 60 min incubation at 37 °C was conducted. As shown in Fig. 4a, the mechanical moduli abruptly increases with temperature and approaches a plateau by incubation at 37 °C for 60 min. The transition of pre-gel solutions to gels occurs when the storage modulus (G′) exceeds the loss modulus (G″) (Kafili et al. 2022). The results indicate that the gelation of pre-gel solutions takes place after a few minutes depending on the dAM concentration (Fig. 4b). The values of storage and loss moduli determine the remarkable effect of dAM concentration on the

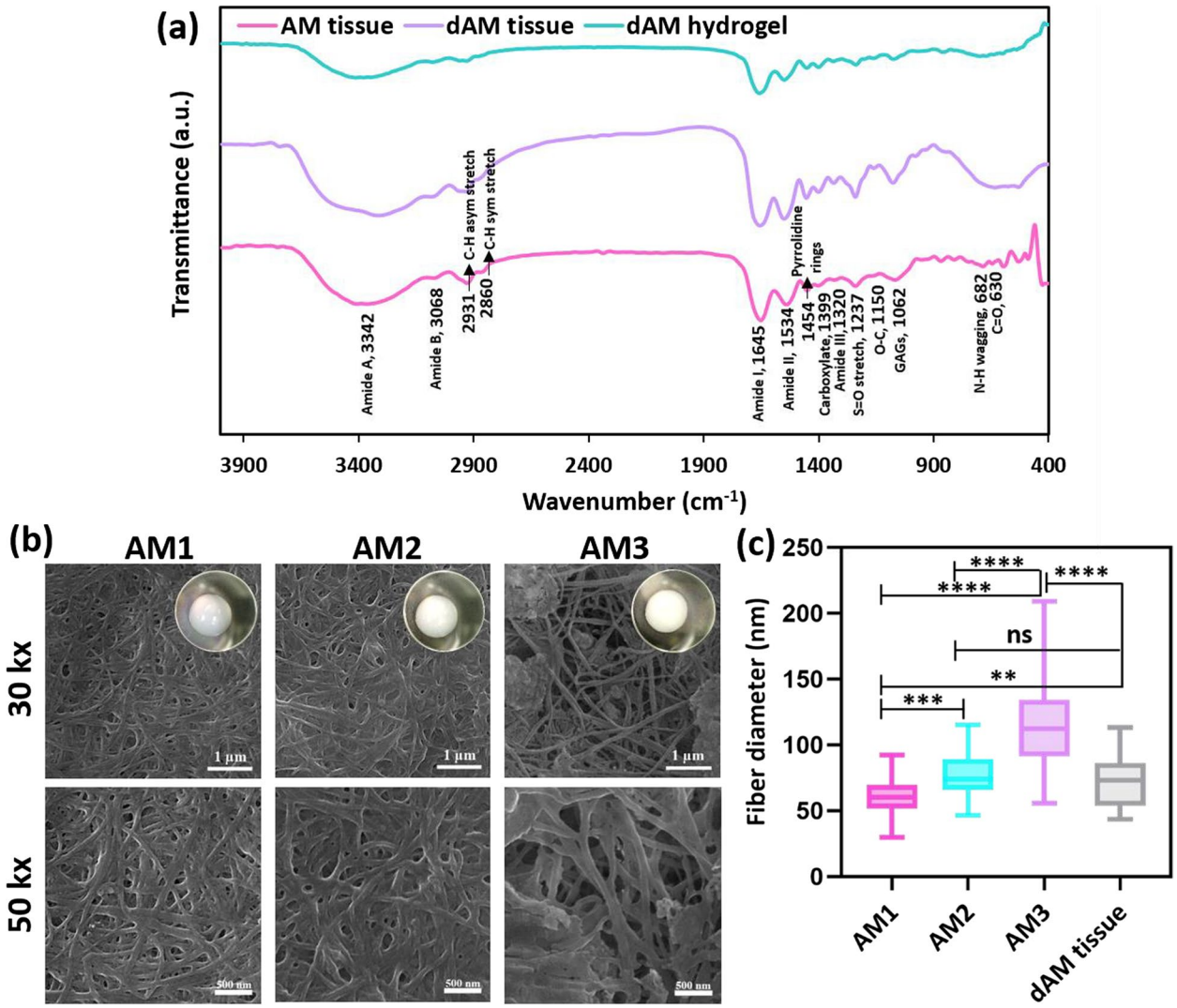

Fig. 3 Compositional and structural characterization of dAM hydrogels with different concentrations. **a** FTIR curves of AM and dAM tissues, and dAM hydrogel (AM2 hydrogel). **b** Representative SEM images of the fibrous structure of dAM hydrogels containing different concentrations of dAM tissue, including 1%w/v (AM1), 2%w/v (AM2), and 3%w/v (AM3), at two different magnifications. Inserts show an electronic image of the prepared hydrogels. **c** Box plot of the fiber size distribution obtained by image analysis of the SEM images ($^{**}p < 0.01$, $^{***}p < 0.001$, $^{****}p < 0.0001$, ns = no significant difference)

mechanical properties, which range from 41.8 ± 2.5 Pa for 1%w/v dAM to 896.2 ± 72.3 Pa for 3%w/v dAM (Fig. 4b). The enhancement of mechanical moduli has also been reported for decellularized tendon-derived bioinks in the concentration range of 5 to 10 mg mL^{-1} and ascribed to the increased density of collagen fibers within the hydrogel matrix (Toprakhisar et al. 2018).

The oscillatory frequency sweep test was conducted on dAM hydrogels after gelation at 37 °C. The changes of mechanical moduli versus frequency show a plateau of up to 10 Hz (Fig. 4c). A slight increase in the moduli at high frequencies (up to 100 Hz) is also noticed. The frequency sweep results confirm the elastic behavior of thermally crosslinked dAM hydrogels regardless of their concentration. An enhancement in the robustness of hydrogels with increasing the dAM concentration is also observed, which is attributed to more crosslinking within the hydrogel networks. Besides, the hydrogels exhibit a shear-thinning behavior (Fig. 4d), which is beneficial for the survival of encapsulated cells during injection from a syringe. The shear-thinning response of dAM hydrogels can be attributed to the easy slipping of collagen subunits upon applying a shear force (Li et al. 2015). With increasing the dAM concentration, the higher number

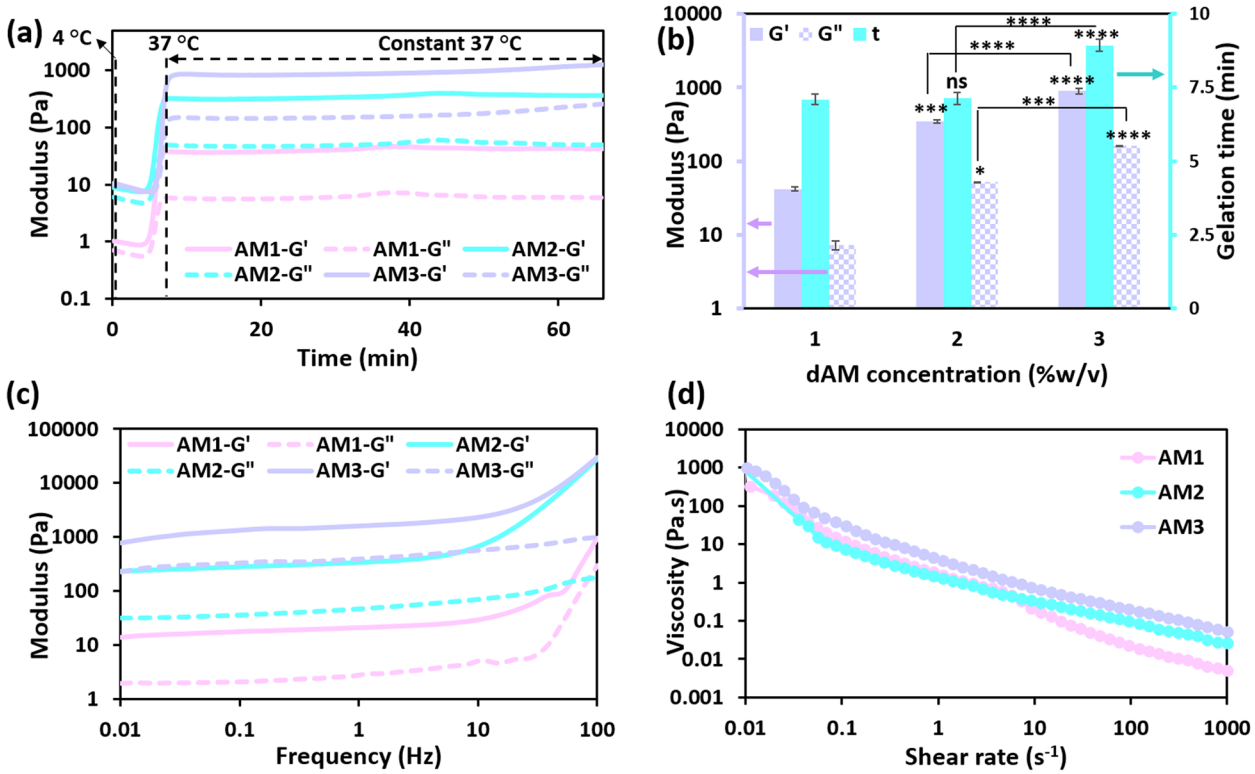

Fig. 4 Rheological behavior of hydrogels containing 1%w/v (AM1), 2%w/v (AM2), and 3%w/v (AM3) dAM content. **a** Temperature ramping from 4 to 37 °C followed by time sweep analysis at the constant temperature of 37 °C. **b** Effect of dAM concentration on the mechanical moduli, including storage modulus (G′) and loss modulus (G″), and gelation time ($^{*}p < 0.05$, $^{***}p < 0.001$, $^{****}p < 0.0001$, ns = no significant difference). **c** Frequency sweep analysis. **d** Viscosity versus shear rate showing the flow behavior

Table 1 Parameters of the power law model fitted on experimental rheological data

Sample name	k (Pa.s^n)	*n*	R^2
AM1	0.69 ± 0.07	0.28 ± 0.02	0.93
AM2	1.23 ± 0.05	0.44 ± 0.01	0.99
AM3	3.03 ± 0.11	0.41 ± 0.01	0.99

of polymeric chains leads to a more viscous hydrogel, resulting in a more compact network with higher inter/intra-molecular friction forces (Ahn et al. 2017).

To better understand the rheological flow behavior, the data were analyzed by the power law model (Eq. 1). The results are summarized in Table 1. As the examined dAM hydrogels exhibit shear-thinning behavior (Fig. 4d), the values of flow index (*n*) are less than 1.0. The *n* index for dAM hydrogel with the concentration of 1%w/v (i.e., AM1) was the lowest among the evaluated range of concentrations, representing a more intense shear-thinning characteristic due to the less physical entanglement and density of collagen fibers. This characteristic can be beneficial for embedded cells within the AM1 hydrogel to withstand exerted shear forces upon injection or extrusion-based bioprinting; however, it may also deteriorate the processability due to uncontrolled ejection of ink material (Ahn et al. 2017). Quantifying the applicability of the developed dAM hydrogels for the fabrication of biomimetic constructs for tissue engineering applications remains a focus of future work. On the other hand, the consistency coefficient (*k*) of hydrogels depends on their viscosity and internal topography (Fan et al. 2022). Therefore, the higher value of *k* in concentrated dAM hydrogels is linked with their viscosity.

A higher hydrogel viscosity is correlated to its better processability, such as enhanced printing quality upon extrusion. Additionally, the higher mechanical strength of the hydrogel improves the shape fidelity and stability of engineered constructs and thus better therapeutic outcomes for treating injured tissues (Saldin et al. 2017; Liu et al. 2024). However, the effect of mechanical tailoring on cellular activities is of great importance, affecting the ultimate functionality of cell-laden tissue-engineered constructs. It is well-documented that the higher rheological and mechanical properties of hydrogels required

for enhanced structural integrity can potentially diminish the viability and functionality of embedded cells (Karamchand et al. 2023). Therefore, the balance between mechanical durability and cell compatibility is a delicate matter that should be considered in developing hydrogels for the 3D culture of biofabricated constructs.

Gelation kinetics

Figure 5a shows the normalized turbidimetric gelation curves of dAM hydrogels. The AM1 hydrogel exhibits a saturation profile with a negligible lag time for gelation. The lag time (t_{lag}) is the delayed time until the beginning of the self-assembly process. The appearance of this gelation behavior is ascribed to the fine fibrous network of the hydrogel construct (Reyna-Valencia et al. 2012), as shown in Fig. 3b. The AM2 and AM3 hydrogels display a typical sigmoidal gelation curve, encompassing the nucleation and growth mechanism of collagen fibrillogenesis (Yang and Kaufman 2009). We propose that the multistep gelation process is initiated by the formation of smaller filament fragments during the lag phase as the nucleus centers. The association of these building blocks into fibrillar bundles through the linear growth phase represents the development of the final equilibrium fibrous network (Tsai et al. 2006). We have also noticed that by increasing the concentration of dAM, the gelation rate is accelerated, although the difference between 2 and 3%w/v is not conspicuous (Fig. 5b). The enhanced gelation rate by increasing the concentration has been reported for tendon-derived bioinks as well (Toprakhisar et al. 2018). Nevertheless, concentrated dAM significantly delays the required time for the formation of filament or microfibrillar nuclei (Fig. 5c), which is in agreement with previous studies (Noitup et al. 2006). Moreover, the time required to reach half of the final turbidity ($t_{1/2}$) is delayed by about 35% when the dAM concentration increases from 1 to 3%w/v (Fig. 5d).

In vitro cell culture

Cell viability, proliferation, and morphology of encapsulated cells in the dAM hydrogels were studied. Figure 6a shows the cytocompatibility of hydrogel extracts examined by indirect MTT assay for up to 7 days. Statistical analyses affirm the non-significant difference between extract-treated cells and those incubated with fresh culture medium (control group). The direct effect of dAM hydrogels on cell viability was evaluated by fluorescence live/dead staining. Herein, the HDF cells were encapsulated in dAM hydrogels with different concentrations and cultured for 7 days. Representative live/dead

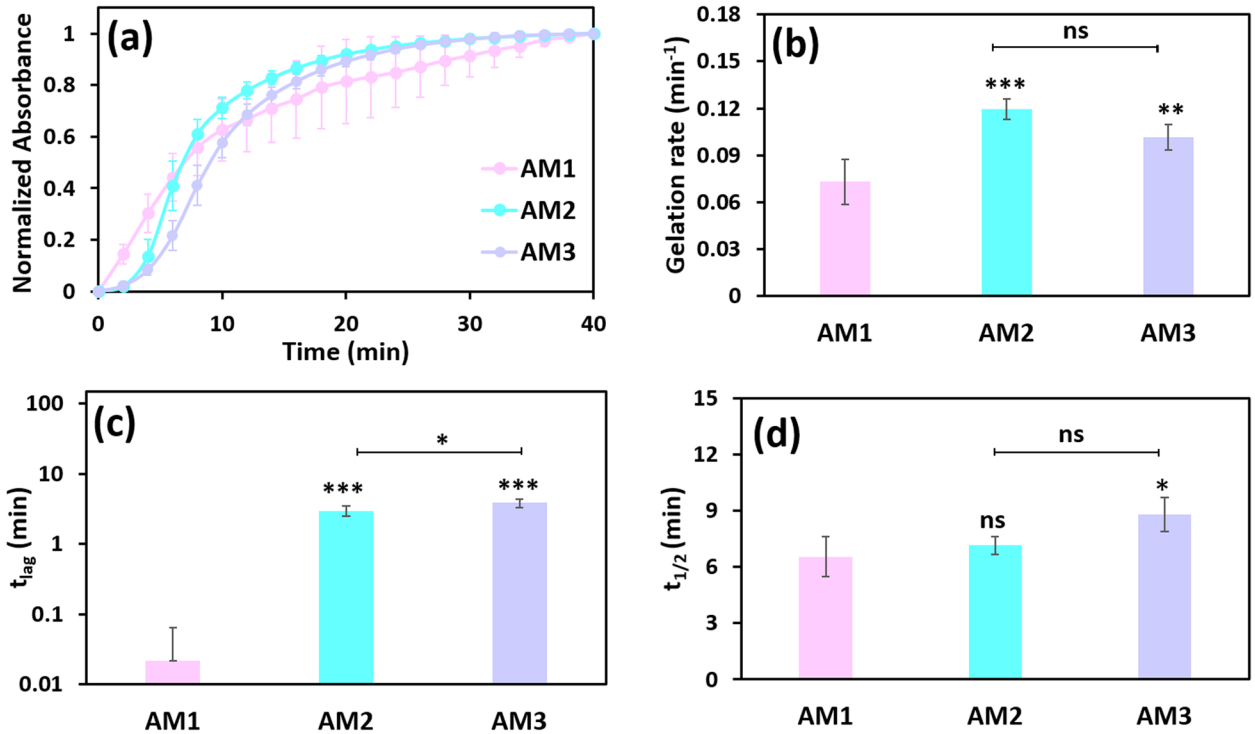

Fig. 5 Effect of dAM concentration (1%w/v (AM1), 2%w/v (AM2), and 3%w/v (AM3)) on the gelation kinetics of hydrogels assessed by turbidimetry method. **a** Normalized turbidimetric curves. The calculated gelation kinetic parameters, including **b** gelation rate, **c** t_{lag}, and **d** $t_{1/2}$ ($^{*}p < 0.05$, $^{**}p < 0.01$, $^{***}p < 0.001$, ns = no significant difference)

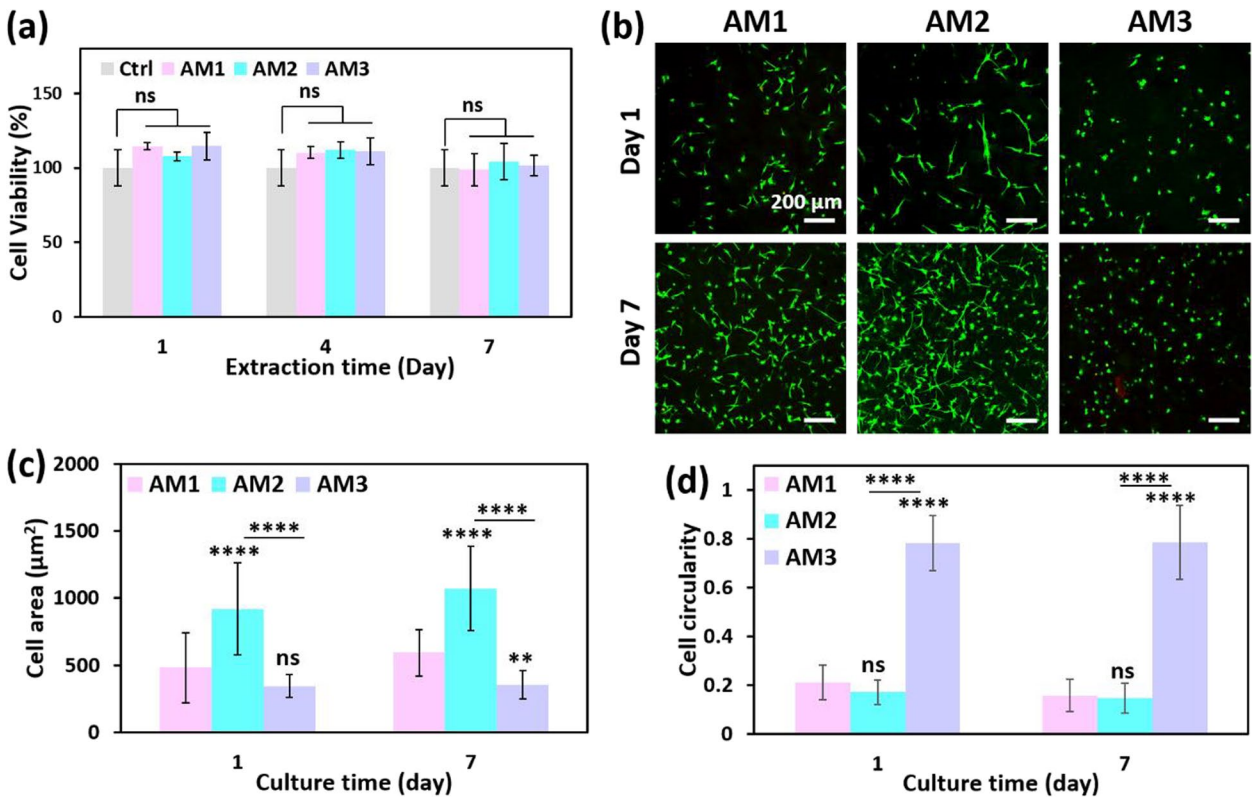

Fig. 6 Cell compatibility of hydrogels with various concentrations of 1%w/v dAM (AM1), 2%w/v dAM (AM2), and 3%w/v dAM (AM3). **a** The cytocompatibility of dAM hydrogels using indirect MTT assay. **b** Fluorescence live (green color)/dead (red color) images of cells encapsulated in dAM hydrogels with different concentrations. **c** Cell spread area. **d** Cell circularity ($^{**}p < 0.01$, $^{****}p < 0.0001$, ns = no significant difference)

images are shown in Fig. 6b. The dAM hydrogel provides a cell-friendly environment for the encapsulated cells, as the cells' majority are alive (green color) even after 7 days. Moreover, the cells encapsulated in dAM hydrogels are proliferative and functional, as evidenced by the increasing population over time. Another interesting outcome of this study is the effect of dAM concentration on the morphology of the encapsulated cells. As shown in Fig. 6b, the fibroblast cells exhibit an elongated spindle morphology inside the hydrogels containing 1 and 2%w/v dAM. However, the cells encapsulated inside the hydrogel containing 3%w/v dAM illustrate an almost spherical shape morphology during the 3D culture period. This variation in the cell morphology could be attributed to different matrix stiffness. Similar results have been reported for human lung fibroblast cells (HFLCs) encapsulated in decellularized lung-derived hydrogels with different concentrations, i.e., fibroblast cells with stretched morphology are found in hydrogels with concentrations less than 20 mg/ml, while spherical cells are obtained in higher concentration (Dabaghi et al. 2021). The cell spreading area and cell circularity after 3D culture are demonstrated in Fig. 6c and d. The fibroblast cells encapsulated in the AM2 hydrogel represent the highest spreading area as well as the lowest circularity index, which corroborates the most stretched morphology of cells. However, statistical analysis determines no significant difference in the circularity of cells in both AM1 and AM2 hydrogels. The cells encapsulated in the AM3 hydrogel possess a high circularity index, confirming their spherical morphology. It should be noted that cell adhesion to dAM hydrogel can mostly be dominated by the cell-binding motifs within the dAM matrix that activate cell–matrix interactions (Bhattacharjee et al. 2020). Of note, our study suggests that the stretching ability of cells to adopt elongated morphology not only depends on their interaction with cell-adhesion motifs but also is affected by the matrix stiffness. This is based on our confocal observations which determine that, regardless of increasing the available amount of cell-binding motifs, the cells exhibit spherical morphology in the AM3 hydrogel with a G′ value of ~ 900 Pa (Fig. 6b).

Discussion

Decellularized ECM-derived hydrogels from different sources of native tissues are considered a bioactive material as a tissue mimetic platform for the development of in vitro tissue models and TE applications (Kort-Mascort et al. 2023). In this study, a pepsin digestion process in a mildly acidic solution was adapted to prepare pre-gel solutions from dAM tissue (Fig. 1). It is known that the cleavage of telopeptide terminal peptides of collagen by the pepsin enzyme can reduce the immunogenic rejection risk of collagen-based biomaterials, such as dAM hydrogels (Lynn et al. 2004). The pH-neutralized pre-gel solutions exhibit a tendency to form a hydrogel by incubation at 37 °C, primarily due to the self-assembly of collagen molecules as the major component of the dAM matrix (Li et al. 2022). The self-assembly of the collagen includes several growth steps initialized by integrating collagen triple helix molecules (thickness of ~ 1.5 nm) followed by the accumulation of these molecular units to build microfibril fragments. The microfibrillar building blocks further rearrange to form collagen fibers with typical diameters of 20 to 80 nm (Cisneros et al. 2006). Our results have revealed that increasing the concentration of dAM leads to the lateral growth of fibrillar bundles by fusing fibrillar units to form fibers with a broader width range (Fig. 3). Therefore, the higher concentration of dAM results in the establishment of more intermolecular crosslinks between collagen monomers to form larger microfibrillar cores (Noitup et al. 2006). Consequently, larger fibrillar cores are formed in hydrogels containing more dAM, while parallel packing of the fibrillar cores during the growth phase forms a reconstructed fibrous network with a high elastic modulus (Fig. 4). Meanwhile, the formation of larger microfibrillar cores requires longer times to initiate gelation (t_{lag}) (Fig. 5c).

The processing of native tissues to a hydrogel through decellularization and digestion process inevitably affects the intrinsic structural architecture of the tissue and diminishes the mechanical strength of dECM-derived hydrogels (Sasikumar et al. 2019). Hence, it is a challenge to tailor the mechanical properties of dECM-derived hydrogels to match the properties of the target application. An approach is the modification of dECM hydrogels by the addition of photo-sensitive moieties (Deus et al. 2022), nanoparticles (Kafili et al. 2022), and synthetic or natural polymers, such as sodium alginate (Kafili et al. 2023c). However, these sorts of alterations are susceptible to compromising the bioactivity of the final hydrogel or even may induce cell toxicity. Alternatively, tailoring dECM hydrogel stiffness by changing concentration can be considered a practical approach for bioprinting and 3D culture applications (Falcones et al. 2021). Therefore, in this study, we have used dAM concentration as the main factor to adjust a range of mechanical stiffness to study cell behaviors.

The effect of 2D culture substrates on cell behavior has been extensively studied and underlying mechanotransduction mechanisms are well documented (Duval et al. 2017). However, the response of cells to 3D hydrogel networks is distinctive of 2D substrates and the morphological features of cells encapsulated in 3D matrixes highly depend on the environmental mechanical stiffness exerted on them. While 2D cell culture may be accompanied by a high proliferation rate and stretched cell morphology (depending on the matrix stiffness), encapsulation of cells in 3D hydrogels requires local degradation of the surrounding microenvironment (Bott et al. 2010). In low- to medium-stiff hydrogels, cells are prone to adhere and present elongated morphology but stiff hydrogels may confine cell stretching by hindering cell mobility. The threshold stiffness value for cells to overcome is highly dependent on the cell type and biophysical characteristics of the chosen matrix materials. For instance, dermal fibroblast cells encapsulated in collagen I-alginate interpenetrating hydrogel networks crosslinked with various concentrations of $CaSO_4$ exhibit morphological paradigm shift at the storage modulus (G') value higher than 320 Pa (e.g., 1200 Pa in this case) (Cunha et al. 2014). Elongated morphology of fibroblasts in PEG-based hydrogels with concentrations of 1.5%w/v ($G' = 241$ Pa) and 2%w/v ($G' = 637$ Pa) are seen while the morphology of cells become spherical at 2.5%w/v concentration ($G' = 1201$ Pa) (Bott et al. 2010). The results of confocal imaging (Fig. 6b) imply that the morphology of cells in soft and medium hydrogels ($G' < 400$ Pa) is elongated while it gets a spherical morphology by increasing the mechanical modulus to $G' > 900$ Pa. A few contractory results have also been reported. For instance, in the work of Bhattacharjee et al., no effect of dAM concentration on the morphology of adipose-derived stem cells (ADSCs) encapsulated in dAM hydrogels (0.2, 0.4, 0.6, and 0.8%w/v all below 1%w/v) has been observed (Bhattacharjee et al. 2020). This observation is most likely due to the lower range of concentration ($\leq$ 1%w/v), and thus mechanical stiffness, which was investigated. In contrast, we have studied a wider range of dAM concentrations with more extensively varying mechanical stiffness. Recently, Deus et al. have prepared photo-crosslinkable dAM hydrogels with various ranges of mechanical properties by altering methacrylated dAM (AdECMMA) concentration and methacrylation degree (Deus et al. 2022). They have shown that the lower concentration of AdECMMA and the lower degree of methacrylation positively influence the viability and elongation of encapsulated human bone marrow-derived mesenchymal stem cells (hBM-MSCs). Although their results open a new path for

the alteration of the dAM hydrogel matrix as the cell culture platform, employing UV light to process the polymer with the Irgacure photoinitiator may cause DNA damage to the encapsulated cells (Xu et al. 2022). Therefore, concentration modification of dAM hydrogels for 3D cell culture provides a healthier microenvironment for cells to function normally as compared to UV-crosslinking.

The dECM derived from AM tissue is a great source of biomaterial with inherent anti-fibrotic, antibacterial, anti-inflammatory, angiogenesis duality, and low immunogenic properties (Kafili et al. 2024b).All these unique properties in this specific biomaterial pave the way for versatile tissue engineering and regenerative medicine (TERM) applications. Due to its multi-functionality, there is a full capacity to exploit dAM hydrogels for the engineering of tissue substitutes to encourage the regeneration of the heart, uterus, skin, cartilage, cornea, etc. (Hu et al. 2023). Consequently, several approaches can be envisioned for the potential usage of dAM hydrogels in TERM applications. For example, the hydrogels can be utilized as an injectable pre-gel solution for minimally invasive therapy to refill the defect area and turn to gel form at body temperature (Henry et al. 2020) (Moreover, they are usable as a source of bioink with encapsulated desired types of cells for the biofabrication of tissue-engineered constructs with intended biomimetic architecture. Furthermore, the dAM hydrogels can be applied as an in vitro platform to study the cell behaviors replicating a pathological condition. Herein, the effect of mechanical tuning of dAM hydrogels as a 3D microenvironment was explored on the morphological characteristics of embedded fibroblast cells. It is noteworthy that fibroblasts are the most frequent cells existing in different tissues, which actively participate in the regeneration process of injured tissues (Sorrell and Caplan 2009) . The transformation between fibroblast sub-populations possessing distinctive morphological features plays a critical role in the early and late stages of regeneration (Zou et al. 2021) Thus, in future studies, the different cell morphologies obtained in this study can be employed to study the function of fibroblast cells in fibrosis or cancer by imitating the complexity of the native diseased microenvironment. In contrast to animal matrixes, a hydrogel-based cell culture platform made of the human dAM is envisioned to be more relevant to human diseases. Particularly, for skin-related issues and/or drug-screening purposes, the human AM is a practical candidate because it resembles the biochemical cues of skin tissue the most (Niknejad et al. 2008). It is also feasible to employ dAM hydrogels as a platform for in vitro studying disease, organ models, mechanistic studies, and drug response evaluations (Harmsen et al. 2023). Overall, the current study provides insights into structural, mechanical, and rheological characteristics of concentration-modulated dAM hydrogels and the possible impacts of these properties on cell responses, such as cell viability and morphology. However, a more profound investigation of gene expression and protein secretion by this cell-embedded in vitro platform requires attention in future studies. These elements can be further correlated to the investigated pathological conditions to study cellular behaviors and functions on the progression of diseases. In addition, the application of dAM hydrogels, as bioink material in advanced biofabrication techniques, has great potential to be pursued in future studies. This approach will open a new pathway to engineer bioinspired constructs to replicate a biomimetic characteristic of the target tissue/organ.

Conclusions

In summary, dAM-derived hydrogels with tunable mechanical properties were prepared via an enzymatic digestion process. It was shown that increasing the dAM concentration (from 1 to 3%w/v) increased the average diameter of collagen fibers (from 56 ± 5.0 to 110.0 ± 14 nm) and enhanced the elastic modulus (from 41.7 ± 2.5 to 896.2 ± 72.3 Pa). In vitro studies determined that the cells were viable and proliferative over 7 days of culture. The dAM hydrogels were used as a biomimetic platform to study cell morphology in 3D networks depending on the matrix stiffness. It was proposed that the morphological features of cultured cells in dAM hydrogels were mostly influenced by the mechanical properties of the matrix. Despite a high amount of available cell-adhesion motifs in the hydrogel containing 3%w/v dAM, the higher stiffness of the platform mechanically confined cell elongation. The hydrogel containing 2%w/v dAM exhibited the highest cell spreading area with spindle-like cell morphology. We have envisaged that dAM hydrogels are not only useable for 3D cell culture but also offer a promising platform for studying cell-related phenomena.

Acknowledgements
The authors thank the Office of Research and Technology of the Sharif University of Technology for providing access to equipment and facilities. The authors would like to thank the support from the School of Medicine, Shahid Beheshti University of Medical Sciences.

Authors' contributions
Golara Kafili: conceptualization, data curation, methodology, investigation, validation, writing an original draft. Elnaz Tamjid: supervision. Hassan Niknejad: supervision. Abdolreza Simchi: conceptualization, supervision, project administration, funding acquisition, resources, writing—review and editing.

Funding
No funding was received for conducting this study.

Availability of data and materials
The raw/processed data required to reproduce these findings are available for sharing upon a reasonable request.

Declarations

Ethics approval and consent to participate

This study was performed in line with the principles of the Declaration of Helsinki. Approval was granted by the Ethics Committee of Shahid Beheshti University of Medical Sciences, Tehran, Iran (ethical code of IR.SBMU.AEC.1402.024).

Consent for publication

The human placentas were collected from consent parents undergoing elective Cesarean delivery at Babak Hospital (Tehran, Iran). Verbal informed consent was obtained from the parents.

Competing interest

The authors declare that they have no competing interests.

Author details

[1]Center for Nanoscience and Nanotechnology, Institute for Convergence Science & Technology, Sharif University of Technology, P.O. Box 14588-89694, Tehran, Iran. [2]Department of Nanobiotechnology, Faculty of Biological Sciences, Tarbiat Modares University, P.O. Box 14115-175, Tehran, Iran. [3]Department of Pharmacology, School of Medicine, Shahid Beheshti University of Medical Sciences, Tehran, Iran. [4]Department of Materials Science and Engineering, Sharif University of Technology, P.O. Box 11365-11155, Tehran, Iran. [5]Center for Bioscience and Technology, Institute for Convergence Science & Technology, Sharif University of Technology, P.O. Box 14588-89694, Tehran, Iran.

Received: 31 May 2024 Accepted: 15 July 2024
Published online: 29 July 2024

References

Ahn G, Min K-H, Kim C et al (2017) Precise stacking of decellularized extracellular matrix based 3D cell-laden constructs by a 3D cell printing system equipped with heating modules. Sci Rep 7(1):1–11. https://doi.org/10.1038/s41598-017-09201-5

Behan K, Dufour A, Garcia O et al (2022) Methacrylated cartilage ECM-based hydrogels as injectables and bioinks for cartilage tissue engineering. Biomolecules 12(2):216. https://doi.org/10.3390/biom12020216

Bhattacharjee M, Ivirico JLE, Kan H-M et al (2020) Preparation and characterization of amnion hydrogel and its synergistic effect with adipose derived stem cells towards IL1β activated chondrocytes. Sci Rep 10(1):18751. https://doi.org/10.1038/s41598-020-75921-w

Bhattacharjee M, Escobar Ivirico JL, Kan H-M et al (2022) Injectable amnion hydrogel-mediated delivery of adipose-derived stem cells for osteoarthritis treatment. Proc Natl Acad Sci 119(4):e2120968119. https://doi.org/10.1073/pnas.2120968119

Bott K, Upton Z, Schrobback K et al (2010) The effect of matrix characteristics on fibroblast proliferation in 3D gels. Biomaterials 31(32):8454–8464. https://doi.org/10.1016/j.biomaterials.2010.07.046

Caliari SR, Burdick JA (2016) A practical guide to hydrogels for cell culture. Nat Methods 13(5):405–414. https://doi.org/10.1038/nmeth.3839

Cavalu S, Roiu G, Pop O et al (2021) Nano-scale modifications of amniotic membrane induced by UV and antibiotic treatment: histological, AFM and FTIR spectroscopy evidence. Materials 14(4):863. https://doi.org/10.3390/ma14040863

Chan G, Mooney DJ (2008) New materials for tissue engineering: towards greater control over the biological response. Trends Biotechnol 26(7):382–392. https://doi.org/10.1016/j.tibtech.2008.03.011

Chao N-N, Li J-L, Ding W et al (2022) Fabrication and characterization of a pro-angiogenic hydrogel derived from the human placenta. Biomaterials Science 10(8):2062–2075. https://doi.org/10.1039/D1BM01891D

Chaudhuri O (2017) Viscoelastic hydrogels for 3D cell culture. Biomaterials Science 5(8):1480–1490. https://doi.org/10.1039/C7BM00261K

Cheng C, Peng X, Qi H et al (2021) A promising potential candidate for vascular replacement materials with anti-inflammatory action, good hemocompatibility and endotheliocyte-cytocompatibility: phytic acid-fixed amniotic membrane. Biomed Mater 16(6):065009. https://doi.org/10.1088/1748-605X/ac246d

Cisneros DA, Hung C, Franz CM et al (2006) Observing growth steps of collagen self-assembly by time-lapse high-resolution atomic force microscopy. J Struct Biol 154(3):232–245. https://doi.org/10.1016/j.jsb.2006.02.006

da Cunha CB, Klumpers DD, Li WA et al (2014) Influence of the stiffness of three-dimensional alginate/collagen-I interpenetrating networks on fibroblast biology. Biomaterials 35(32):8927–8936. https://doi.org/10.1016/j.biomaterials.2014.06.047

Dabaghi M, Saraei N, Carpio MB et al (2021) A robust protocol for decellularized human lung bioink generation amenable to 2D and 3D lung cell culture. Cells 10(6):1538. https://doi.org/10.3390/cells10061538

Deus IA, Santos SC, Custódio CA et al (2022) Designing highly customizable human based platforms for cell culture using proteins from the amniotic membrane. Biomaterials Advances 134:112574. https://doi.org/10.1016/j.msec.2021.112574

Doudi S, Barzegar M, Taghavi EA, et al (2022) Applications of acellular human amniotic membrane in regenerative medicine. Life Sci. 121032. https://doi.org/10.1016/j.lfs.2022.121032

Duval K, Grover H, Han LH et al (2017) Modeling physiological events in 2D vs. 3D cell culture. Physiology 32(4):266–277. https://doi.org/10.1152/physiol.00036.2016

Falcones B, Sanz-Fraile H, Marhuenda E et al (2021) Bioprintable lung extracellular matrix hydrogel scaffolds for 3D culture of mesenchymal stromal cells. Polymers 13(14):2350. https://doi.org/10.3390/polym13142350

Fan Z, Cheng P, Zhang P et al (2022) A novel multifunctional Salecan/κ-carrageenan composite hydrogel with anti-freezing properties: advanced rheology, thermal analysis and model fitting. Int J Biol Macromol 208:1–10. https://doi.org/10.1016/j.ijbiomac.2022.03.054

Fernández-Pérez J, Ahearne M (2019) The impact of decellularization methods on extracellular matrix derived hydrogels. Sci Rep 9(1):1–12. https://doi.org/10.1038/s41598-019-49575-2

Harmsen MC, Getova V, Zhang M, et al (2023) Organ-derived extracellular matrix (ECM) hydrogels: versatile systems to investigate the impact of biomechanics and biochemistry on cells in disease pathology. Handbook of the Extracellular Matrix: Biologically-Derived Materials: Springer. 1–27. https://doi.org/10.1007/978-3-030-92090-6_43-1

Henry JJ, Delrosario L, Fang J et al (2020) Development of injectable amniotic membrane matrix for postmyocardial infarction tissue repair. Adv Healthcare Mater 9(2):1900544. https://doi.org/10.1002/adhm.201900544

Hu Z, Luo Y, Ni R, et al (2023) Biological importance of human amniotic membrane in tissue engineering and regenerative medicine. Materials Today Bio. 100790. https://doi.org/10.1016/j.mtbio.2023.100790

Johnson TD, Lin SY, Christman KL (2011) Tailoring material properties of a nanofibrous extracellular matrix derived hydrogel. Nanotechnology 22(49):494015. https://doi.org/10.1088/0957-4484/22/49/494015

Jones BC, Elvassore N, De Coppi P, et al (2022) Extracellular matrix hydrogels from decellularized tissues for biological and biomedical applications. Multifunctional Hydrogels for Biomedical Applications. 1–22. https://doi.org/10.1002/9783527825820.ch1

Kafili G, Tamjid E, Niknejad H et al (2022) Development of injectable hydrogels based on human amniotic membrane and polyethyleneglycol-modified nanosilicates for tissue engineering applications. Eur Polymer J 179:111566. https://doi.org/10.1016/j.eurpolymj.2022.111566

Kafili G, Kabir H, Jalali Kandeloos A et al (2023a) Recent advances in soluble decellularized extracellular matrix for heart tissue engineering and organ modeling. J Biomater Appl 38(5):577–604. https://doi.org/10.1177/08853282231207216

Kafili G, Tamjid E, Niknejad h et al (2023b) Effect of pepsin digestion time on the properties of temperature sensitive human amniotic membrane derived hydrogel. Modares J Biotechnol. 13(3):113–131. http://biot.modares.ac.ir/article-22-51635-fa.html

Kafili G, Tamjid E, Niknejad H et al (2023c) Development of printable nanoengineered composite hydrogels based on human amniotic membrane for wound healing application. J Mater Sci 58(30):12351–12372. https://doi.org/10.1007/s10853-023-08783-y

Kafili G, Tamjid E, Niknejad H et al (2024a) Development of bioinspired nanocomposite bioinks based on decellularized amniotic membrane and hydroxyethyl cellulose for skin tissue engineering. Cellulose 31(4): 2989-3013. https://doi.org/10.1007/s10570-024-05797-w

Kafili G, Niknejad H, Tamjid E et al (2024b) Amnion-derived hydrogels as a versatile platform for regenerative therapy: from lab to market. Frontiers

in Bioengineering and Biotechnology 12:1358977. https://doi.org/10.3389/fbioe.2024.1358977
Karamchand L, Makeiff D, Gao Y et al (2023) Biomaterial inks and bioinks for fabricating 3D biomimetic lung tissue: a delicate balancing act between biocompatibility and mechanical printability. Bioprinting 29:e00255. https://doi.org/10.1016/j.bprint.2022.e00255
Kort-Mascort J, Flores-Torres S, Chavez OP et al (2023) Decellularized ECM hydrogels: prior use considerations, applications, and opportunities in tissue engineering and biofabrication. Biomaterials Science. https://doi.org/10.1039/D2BM01273A
Li C, Duan L, Tian Z et al (2015) Rheological behavior of acylated pepsin-solubilized collagen solutions: effects of concentration. Korea-Australia Rheology Journal 27(4):287–295. https://doi.org/10.1007/s13367-015-0028-6
Li X, Li P, Wang C et al (2022) A thermo-sensitive and injectable hydrogel derived from a decellularized amniotic membrane to prevent intrauterine adhesion by accelerating endometrium regeneration. Biomaterials Science 10(9):2275–2286. https://doi.org/10.1039/D1BM01791H
Liu H, Xing F, Yu P, et al (2024) Biomimetic fabrication bioprinting strategies based on decellularized extracellular matrix for musculoskeletal tissue regeneration: current status and future perspectives. Materials & Design. 113072. https://doi.org/10.1016/j.matdes.2024.113072
Lynn A, Yannas I, Bonfield W (2004) Antigenicity and immunogenicity of collagen. Journal of Biomedical Materials Research Part b: Applied Biomaterials: an Official Journal of the Society for Biomaterials, the Japanese Society for Biomaterials, and the Australian Society for Biomaterials and the Korean Society for Biomaterials 71(2):343–354. https://doi.org/10.1002/jbm.b.30096
Nieto D, Marchal Corrales JA, Jorge de Mora A, et al (2020) Fundamentals of light-cell–polymer interactions in photo-cross-linking based bioprinting. APL bioengineering. 4(4). https://doi.org/10.1063/5.0022693
Niknejad H, Peirovi H, Jorjani M et al (2008) Properties of the amniotic membrane for potential use in tissue engineering. Eur Cells Mater 15:88–99. https://doi.org/10.22203/ecm
Noitup P, Morrissey MT, Garnjanagoonchorn W (2006) In vitro self-assembly of silver-line grunt type I collagen: effects of collagen concentrations, pH and temperatures on collagen self-assembly. J Food Biochem 30(5):547–555. https://doi.org/10.1111/j.1745-4514.2006.00081.x
Peak CW, Stein J, Gold KA et al (2018) Nanoengineered colloidal inks for 3D bioprinting. Langmuir 34(3):917–925. https://doi.org/10.1021/acs.langmuir.7b02540
Peng X, Wang X, Cheng C et al (2020) Bioinspired, artificial, small-diameter vascular grafts with selective and rapid endothelialization based on an amniotic membrane-derived hydrogel. ACS Biomater Sci Eng 6(3):1603–1613. https://doi.org/10.1021/acsbiomaterials.9b01493
Pouliot RA, Young BM, Link PA et al (2020) Porcine lung-derived extracellular matrix hydrogel properties are dependent on pepsin digestion time. Tissue Eng Part C Methods 26(6):332–346. https://doi.org/10.1089/ten.tec.2020.0042
Ravichandran A, Murekatete B, Moedder D et al (2021) Photocrosslinkable liver extracellular matrix hydrogels for the generation of 3D liver microenvironment models. Sci Rep 11(1):15566. https://doi.org/10.1038/s41598-021-94990-z
Reyna-Valencia A, Chevallier P, Mantovani D, editors (2012) Development of a collagen/clay nanocomposite biomaterial. Materials Science Forum. Trans Tech Publ. https://doi.org/10.4028/www.scientific.net/MSF.706-709.461
Rothrauff BB, Coluccino L, Gottardi R et al (2018) Efficacy of thermoresponsive, photocrosslinkable hydrogels derived from decellularized tendon and cartilage extracellular matrix for cartilage tissue engineering. J Tissue Eng Regen Med 12(1):e159–e170. https://doi.org/10.1002/term.2465
Ryzhuk V, Zeng XX, Wang X et al (2018) Human amnion extracellular matrix derived bioactive hydrogel for cell delivery and tissue engineering. Mater Sci Eng C 85:191–202. https://doi.org/10.1016/j.msec.2017.12.026
Saldin LT, Cramer MC, Velankar SS et al (2017) Extracellular matrix hydrogels from decellularized tissues: structure and function. Acta Biomater 49:1–15. https://doi.org/10.1016/j.actbio.2016.11.068
Sasikumar S, Chameettachal S, Cromer B et al (2019) Decellularized extracellular matrix hydrogels—cell behavior as a function of matrix stiffness. Current Opinion in Biomedical Engineering 10:123–133. https://doi.org/10.1016/j.cobme.2019.05.002
Sorrell JM, Caplan AI (2009) Fibroblasts—a diverse population at the center of it all. Int Rev Cell Mol Biol 276:161–214. https://doi.org/10.1016/S1937-6448(09)76004-6
Sripriya R, Kumar R (2016) Denudation of human amniotic membrane by a novel process and its characterisations for biomedical applications. Prog Biomater 5:161–172. https://doi.org/10.1007/s40204-016-0053-7
Tian H, Ren Z, Shi L et al (2021) Self-assembly characterization of tilapia skin collagen in simulated body fluid with different salt concentrations. Process Biochem 108:153–160. https://doi.org/10.1016/j.procbio.2021.06.013
Toniato TV, Stocco TD, Martins DdS et al (2020) Hybrid chitosan/amniotic membrane-based hydrogels for articular cartilage tissue engineering application. Int J Polym Mater Polymeric Biomaterials 69(15):961–970. https://doi.org/10.1080/00914037.2019.1636249
Toprakhisar B, Nadernezhad A, Bakirci E et al (2018) Development of bioink from decellularized tendon extracellular matrix for 3D bioprinting. Macromol Biosci 18(10):1800024. https://doi.org/10.1002/mabi.201800024
Tsai SW, Liu RL, Hsu FY et al (2006) A study of the influence of polysaccharides on collagen self-assembly: nanostructure and kinetics. Biopolymers: Original Research on Biomolecules 83(4):381–388. https://doi.org/10.1002/bip.20568
Villamil Ballesteros AC, Segura Puello HR, Lopez-Garcia JA et al (2020) Bovine decellularized amniotic membrane: extracellular matrix as scaffold for mammalian skin. Polymers 12(3):590. https://doi.org/10.3390/polym12030590
Xu H-Q, Liu J-C, Zhang Z-Y et al (2022) A review on cell damage, viability, and functionality during 3D bioprinting. Mil Med Res 9(1):70. https://doi.org/10.1186/s40779-022-00429-5
Yang Y-l, Kaufman LJ (2009) Rheology and confocal reflectance microscopy as probes of mechanical properties and structure during collagen and collagen/hyaluronan self-assembly. Biophys J 96(4):1566–1585. https://doi.org/10.1016/j.bpj.2008.10.063
Zhang L, Zou D, Li S et al (2016) An ultra-thin amniotic membrane as carrier in corneal epithelium tissue-engineering. Sci Rep 6(1):1–12. https://doi.org/10.1038/srep21021
Zhang W, Du A, Liu S et al (2021a) Research progress in decellularized extracellular matrix-derived hydrogels. Regenerative Therapy 18:88–96. https://doi.org/10.1016/j.reth.2021.04.002
Zhang Q, Chang C, Qian C et al (2021b) Photo-crosslinkable amniotic membrane hydrogel for skin defect healing. Acta Biomater 125:197–207. https://doi.org/10.1016/j.actbio.2021.02.043
Zou M-L, Teng Y-Y, Wu J-J et al (2021) Fibroblasts: heterogeneous cells with potential in regenerative therapy for scarless wound healing. Frontiers in Cell and Developmental Biology 9:713605. https://doi.org/10.3389/fcell.2021.713605

Publisher's Note

Springer Nature remains neutral with regard to jurisdictional claims in published maps and institutional affiliations.